ULTRASONIC RAIL FLAW TESTING PARAMETERS IN EXTREME COLD TEMPERATURE

for Transport Canada

Prepared by Anish Poudel, Survesh Shrestha,
Brian Lindeman, MxV Rail
Glenn Washer, University of Missouri

Proprietary Report

P-22-018

October 24, 2022

MxV Rail (formerly TTCI)
A subsidiary of the Association of American Railroads
350 Keeler Parkway | Pueblo, Colorado USA 81001
www.mxvrail.com

Executive Summary

This report summarizes MxV Rail (formerly TTCI) findings on the ultrasonic testing (UT) parameters with an emphasis on the impact of cold temperatures related to non-stop ultrasonic rail flaw testing. To assess and quantify the performance of the UT nondestructive evaluation (NDE) method in extreme cold temperatures, ultrasonic velocity and density in rail steel and different fluids (couplants) were first determined by conducting experiments in the laboratory. Changes in refraction angle (shear waves) were also measured during the experiments. All experiments were conducted using a chiller bath inside an ultrasonic immersion tank for non-contact UT tests and using a cold chamber for the contact UT tests. For the non-contact test, the couplants used included glycol and EchoPure™ gel. The glycol was also mixed with water to create different concentrations, e.g., 80/20 mix and 50/50 mix. Similarly, delay lines were manufactured to provide a buffer against the cold temperatures that will be experienced during the non-contact testing. A stainless-steel collar was fabricated to fix the delay line to the front of the transducer, and suitable pressure was applied to enable the efficient transfer of acoustic energy. Echo Ultrasonics® Forever Wedge ultrasonic couplant was used to connect the delay line to the transducer. Finally, the ultrasonic velocity and density obtained from the experimentation was used in the ultrasonic beam modeling and simulation in rails. Some of the key findings of this research include:

Contact UT Tests:

- Average L-wave velocity determined at room temperature was 5,865 meter per second (m/s) and at -38°C was 5,878 m/s. This corresponds with a 0.22 percent change of average L-wave velocity and a linear velocity increase trend.
- Average S-wave (45°) velocity determined at room temperature was 3,255 m/s and at -38°C was 3,340 m/s. This corresponds with a 2.61 percent change of average L-wave velocity and a linear velocity increase trend.
- Average S-wave (70°) velocity determined at room temperature was 3,251 m/s and at -38°C was 3,304 m/s. This corresponds with a 1.65 percent change of average L-wave velocity and a linear velocity increase trend.
- Data scatter was observed during most of the velocity measurements. These velocity measurements were result of amplitude shifts (erratic readings) of the recorded A-scans. The amplitude shifts in A-scans may be due to the changes in the piezoelectric crystal properties due to prolonged exposure to the lower temperature. Similar trends were observed in outside research for the high temperature testing. Future research will need to be performed to better understand how the cold temperature affects the UT A-scan amplitudes.

Non-Contact UT Tests

- Ultrasonic velocity increased with decreasing temperature for all fluids tested. All velocity measurements followed the same linear trend (increasing) with the decrease in temperature.
- L-wave velocities for rail steel were measured from 23°C to only -30°C. Temperatures below -30°C were not achievable in the chiller batch.
- L-wave velocity measurements for rail steel at temperatures of -20°C, -25°C, and -30°C were not consistent with the overall trend velocity increasing as temperature decrease. This may

have been due to the increased ultrasonic signal losses in the liquid resulting in reduced signal-to-noise-ratio (SNR) leading to timing errors in the received signal. The average L-wave velocity determined at room temperature was 5,859 m/s and at -30°C was 5,880 m/s, and it corresponds to a velocity increase of 0.55 m/sec/°C.

- The procedure used for a 45° S-wave was effective but again proved problematic for 70° S-waves due to ultrasonic signal losses in the immersion liquid (80/20 glycol/water) as temperatures decreased.
- Average S-wave (45°) velocity determined at room temperature was 3,212 m/s, at -20°C was 3,224 m/s, and at -30°C was 3,229 m/s. This corresponds to velocity increase approximately 0.37 m/sec/°C.
- A 45° refraction angle change as a function of temperature was found to be 0.0782°C, and the relationship was found to be linear.
- Signal attenuation losses in the steel increased at the lower temperature. For example, losses in amplitude were shown to be about -0.21 decibels/millimeter (dB/mm) at -20°C as compared with -0.19 dB/mm at -5°C. The phenomena of increased attenuation in both the rail steel and the liquid couplant may be worthy of further study. Very little data is available in the literature to document this effect. Practically, the ultrasonic signal losses will impact damage detection in the field by reducing the amplitude of signals as compared to a threshold value identified to determine if a given signal represents a reportable indication. Signal attenuation losses were developed from the data on ultrasonic velocities; additional detailed testing is needed to characterize attenuation changes as a function of temperature.
- The experimental results reported here were developed from the data on ultrasonic velocities; additional detailed testing is needed to characterize attenuation changes as a function of temperature.

UT Beam Modeling and Simulation

- Ultrasonic beam modeling and simulation was conducted to assess ultrasonic beam field responses for the range of ultrasonic velocities and densities determined for different cold temperatures.
- The velocity of sound waves in different materials governs the angle of refraction when a wave is transmitted from one material to the other, and this effect was evident in the modeling as well as the experimental measurement described above. The refraction angle shows a decreasing linear trend with a linear regression value of 0.98 for both cases. This shift in the angle of refraction can cause the beam to shift away from the targeted inspection zone, a shift that can cause the beam to possibly miss defects in that zone during the inspection process. Based on this possibility of shift, it is highly recommended that hi-rail ultrasonic system calibration is conducted at cold temperatures when performing testing at cold temperatures.
- Except for the water/steel simulation at room temperature, all other simulations conducted for extreme low temperatures failed to detect transverse type defects as a result of the change in the refraction angle.

Table of Contents

List of Figures

List of Tables

1.0 INTRODUCTION

Transport Canada's (TC) Innovation Centre (IC) awarded MxV Rail (formerly TTCI), a wholly owned subsidiary of the Association of American Railroads (AAR), a Phase II contract to continue researching "cold climate railway technologies." The goal of this research is to understand the effect of extreme cold climate on railway infrastructure and maintenance and address planned and unforeseen issues related to extreme winter weather operations in the Canadian railroad environment. Working in conjunction with the project steering committee (comprised of program officers from TC's IC, rail safety experts, and the railroad industry) and in consultation with stakeholders and technical experts from the Railway Research Advisory Board (RRAB), two research topics were identified and proposed for this phase. This report summarizes the findings on the ultrasonic testing parameters, emphasizing the impact of cold temperatures in relation to non-stop ultrasonic rail flaw testing.

1.1 Background

Minute anomalies or defects can act as initialization sites for internal rail cracks that can grow with accumulated train tonnage.[1-3] Rail defects come in variety of forms (shape, sizes, location, and orientation) and are well described in the Federal Railroad Administration (FRA) rail defect manual as well as in various railroads and rail service providers' rail defect manuals. Broken rails and welds due to internal flaws, defects, and/or anomalies poses significant challenges for railroads and those operating in extreme cold weather conditions.[4] It is commonly believed that one of the main reasons for increased broken rails in the extreme cold winter is mainly due to the rail temperature decreasing by a significant amount from the rail neutral temperature causing rails to experience high tensile force[5] and subsequent failure at weak spots, such as at fatigue defects that form inside the rails and welds.

North American Class I railroads rely primarily on the use of ultrasonic testing (UT) nondestructive evaluation (NDE) technology to detect and characterize rail defects at a regular interval. However, even with such advanced NDE technology, some defects are only discovered after the rail breaks.[6] Therefore, improving railroad safety through the reduction of rail failures and the associated risks of train accidents, while achieving higher reliability with ultrasonic NDE inspection for rail flaw detection and characterization, is the main goal of rail defect detection.

1.2 Ultrasonic Rail Flaw Testing

The in-motion UT technology for rail flaw testing is usually implemented on a hi-rail vehicle platform (commonly referred to as "rail detector cars"). These cars use fixed-angle piezoelectric transducers housed in a liquid-filled membrane (tire) called a roller search unit (RSU) to generate/emit ultrasonic waves in the rail. Figure 1 shows a typical RSU configuration running on the rail. Ray trace is displayed as a single line but, in reality, an array of the ultrasonic beam is transmitted and received. Similarly, Table 1 shows different types of transducers used for finding different types of rail internal defects.

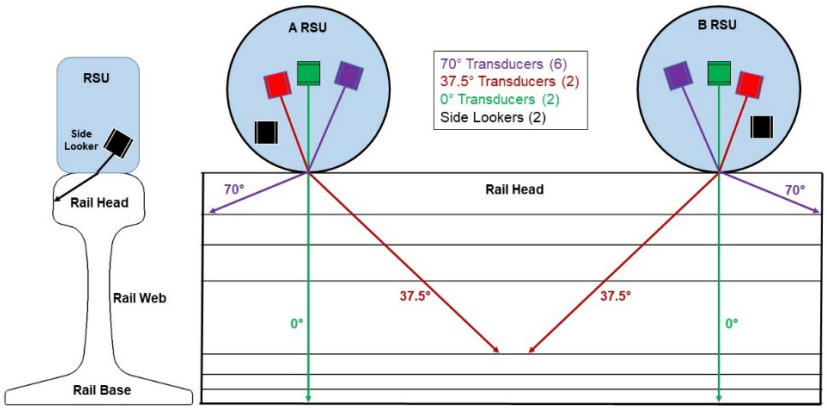

Figure 1. Ultrasonic transducers configurations in RSUs[6]

Table 1. Transducer orientation and targeted flaw types[6]

Transducer Types	Target Flaw Types
0°	Flaws oriented horizontally [shells, horizontal split head (HSH), split web]
37.5° or 45°	Bolt hole cracks, web defects
70°	Transverse defects (TDs), vertical split heads (VSH) weld defects (porosity, inclusions, etc.)

The peak testing speed with rail detector cars can exceed 30 kilometers per hour (km/h) on North American railroads, but the start-stop "hand verify" operation often limits average test speeds to around 12 km/h.[6] However, inspection speeds in some other countries are reported to be as high as 100 km/h.[7, 8] In many of these cases, a detector car does not stop to further hand verify indications. The inspection data is recorded and analysed later in the back office, but, for North American Class I railroads, the start-stop hand verifying operation requires NDE operators to stop the detector car, step down from the vehicle, and manually hand verify flaws in the rail using the portable ultrasonic system to see if any relevant indication is detected. Hand verification is usually done to confirm a detector car finding and size the defect so proper remedial action can be taken.

The United States Department of Transportation (USDOT) FRA now also allows North American railroads to conduct continuous rail testing using ultrasonic technology augmented with GPS technology. In this approach, rail inspection equipment is able to collect and transmit inspection data nonstop to remote locations for detailed analysis.[9] If a suspected defect is verified, FRA regulations require the railroad to apply the proper remedial action immediately. In some cases, the proper remedial action means repairing or replacing the defective rail, slowing trains over the defect, or removing the track from service to stop trains until repairs can be made.[10]

2.0 PROJECT OBJECTIVE AND SCOPE

The main objective of this research was to investigate and understand the effectiveness of ultrasonic rail flaw testing in extreme cold weather conditions, as it relates to continuous testing as well as traditional rail flaw testing. The following tasks were performed to assess and quantify the performance of this technique in such extreme cold temperatures:

- Determination of ultrasonic velocity in rail steel and the velocity and density of coupling fluids.
- Ultrasonic beam modeling and simulation in rails.

3.0 ULTRASONIC PARAMETERS

For effective transfer of the ultrasonic energy into the rail steel and back to transducers, roller search units (RSUs) are usually filled with fluids that have a minimal variation of ultrasonic velocity with temperature. In addition, fluid and the RSU material are chosen in order to minimize acoustic impedance mismatch. Acoustic impedance (Z) is a physical material property that depends on the density (ρ) and acoustic velocity (C) of the material described by Equation 1.[11]

$$Z = \rho C \quad (1)$$

The effect of acoustic impedance on ultrasonic inspection becomes noticeable at interfaces between different material types. The ability of ultrasound to transfer from one material type to another material type also depends on the acoustic impedance difference between two materials. If the difference in impedance between the two materials is significant, then most of the sound wave is reflected.

Also, one of the key things to consider while conducting ultrasonic inspection is the ambient temperature at which the tests are being conducted because the acoustic velocity in material depends on the stiffness and density of the material. The dependence of ultrasonic wave velocities on temperature is well described by following equation:[11]

$$C_l = \sqrt{\frac{K}{\rho}} \; and \; C_s = \sqrt{\frac{G}{\rho}} \quad (2)$$

Where:

K is the bulk modulus,

G is the shear modulus, and

C_l and C_s are the longitudinal and shear wave velocity.

From Equation 2, it is evident that the acoustic velocity in material can be affected by the change in the density of material. Density changes with temperature because volume changes with temperature, i.e., when the temperature increases, density reduces and vice versa. Similarly. the velocity of sound wave can be also calculated by using Equation 3.

$$C = \frac{2d}{t} \quad (3)$$

Where:

d is the thickness of sample, and

t is the transit time of ultrasonic wave.

From these equations, it can be inferred that the sound waves travel faster through media with higher stiffness and/or lower density. If a medium is not compressible at all (incompressible), the speed of sound can be infinite ($C \approx \infty$).

Similarly, when an ultrasonic wave passes through an interface between two materials at an oblique angle, both reflected and refracted waves are produced. Due to the different velocities of the acoustic waves within the two materials, refraction takes place at an interface as shown in Figure 2. When ultrasonic waves enter a medium with a larger index of refraction (n), the waves bend toward the direction that is normal to the surface.

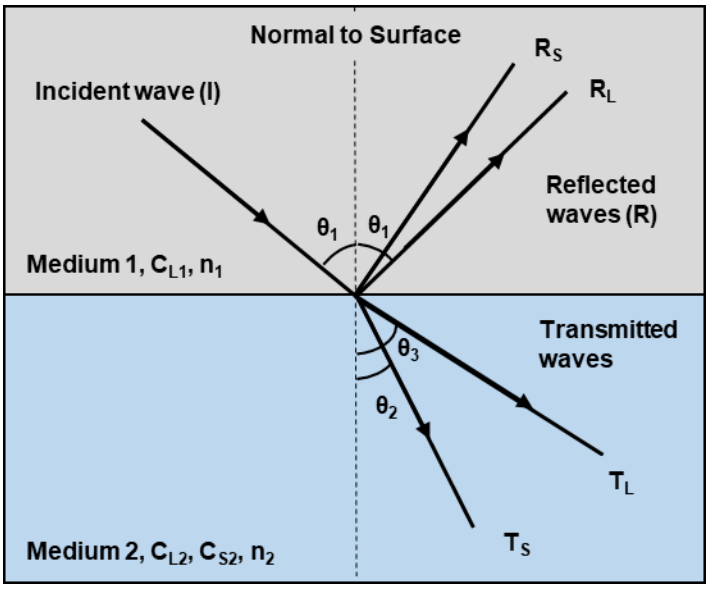

Figure 2. Mode conversion at interface for longitudinal wave incidence

Snell's Law usually describes the relationship between the angles and the velocities of the ultrasonic waves in different mediums and is given by:[12]

$$\frac{\sin\theta_1}{C_{l1}} = \frac{\sin\theta_3}{C_{l2}} = \frac{\sin\theta_2}{C_{s2}} = \frac{n_2}{n_1} \qquad (4)$$

4.0 EXPERIMENTAL SETUPS

Two different experimental setups were designed and conducted to measure the ultrasonic parameters for this research. The first test setup included experiments for measuring ultrasonic velocity using the contact UT approach. Similarly, the second test setup involved experiments for measuring ultrasonic velocity, density, and angle of refraction using a non-contact UT approach as it relate to continuous rail testing. Although non-contact UT test setups were

designed to mimic extreme winter revenue service type scenarios, some limitations were encountered while conducting these tests in the laboratory. To name a few limitations, instead of using RSU, a delay line transducer was used to generate ultrasonic waves, and all tests were done at the static conditions as opposed to dynamic conditions in the actual rail testing environment. Nevertheless, these tests provided greater insights and a broader understanding into some of the key UT parameters for extreme cold weather conditions.

4.1 Contact UT Test Setup

A test block was machined from the head of a 136RE rail to conduct velocity measurements. The dimensions of the fabricated sample were 203 mm x 25 mm x 51 mm. A 3 mm diameter through hole was also drilled at the center of the test block. Figure 3 shows the engineering drawing of the fabricated test block.

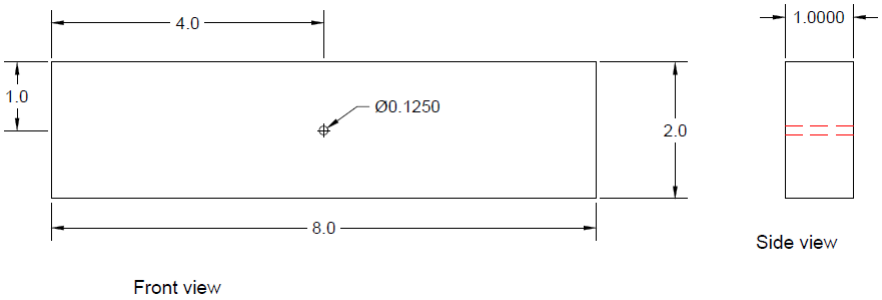

Figure 3. Engineering drawing of the test block. Dimensions shown are in inches

Figure 4 shows the contact UT test setup in the laboratory using an environmental cold chamber. This cold chamber enabled measurements down to -38°C. EchoPure™ water-free, medium viscosity couplant was used during the testing. A thermocouple was attached to the surface of the test sample to monitor its temperature. Also, clamps were used to hold the transducer to the rail steel for ultrasonic measurements at lower temperatures. These measurements were conducted using both longitudinal wave (L-wave) and shear wave (S-wave) (45° and 70°) transducers.

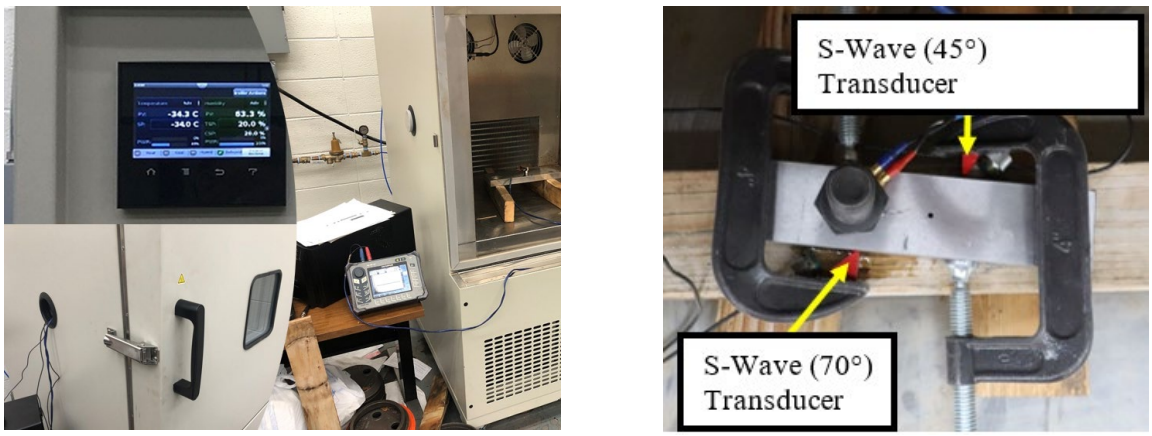

Figure 4. Cold temperature laboratory test setup for velocity measurements in rail steel using contact UT approach

4.2 Non-Contact UT Test Setup

For the non-contact UT setup, ultrasonic measurements in rail steel and couplants (fluids) were conducted by placing a chiller bath inside an ultrasonic immersion tank. Although the chiller used had a specified rated minimum temperature of -50°C, the actual minimum temperature that could be achieved in the laboratory was about -37°C. Figure 5 shows the test setup used for measuring the ultrasonic parameters using a non-contact UT approach. As shown in the figure, the specimen was enclosed within an aluminium container within the chiller bath. The glycol/water mixture within the chiller bath itself was opaque due to the entrapped air bubbles generated by the circulating pump in the chiller bath. The aluminium container enclosing the specimen was needed because the entrapped air bubbles in the immersion liquid caused a scattering of ultrasonic waves, thereby reducing the energy in the ultrasonic waves significantly.

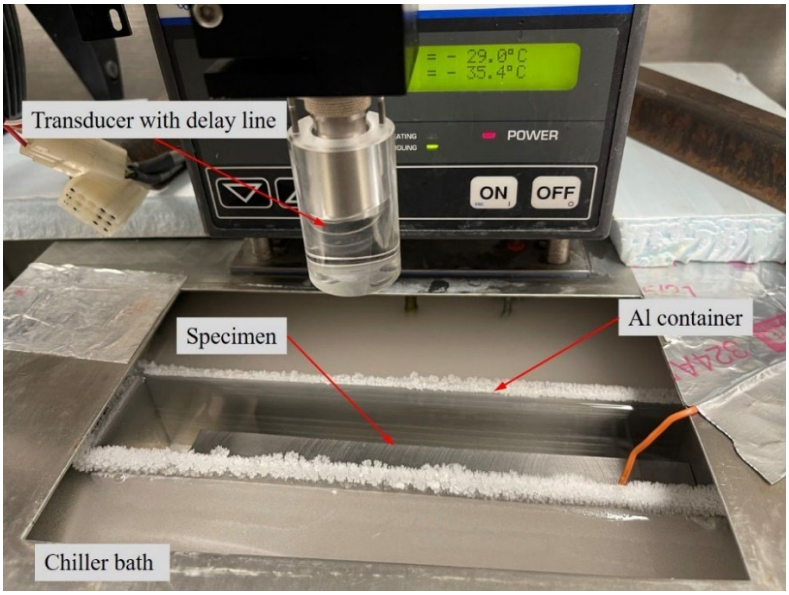

Figure 5. Cold temperature laboratory test setup for velocity measurements in rail steel and fluids using non-contact UT approach

4.2.1 Calibration Specimen

A calibration specimen was machined from a piece of 136RE rail steel. The specimen was sectioned from the head and web area of the rail. The geometry of the specimen is shown in Figure 6. The specimen was fabricated with a 51 mm radius and three 1.5 mm side-drilled holes (SDH) at depths of 13, 25, and 38 mm from the surface of the specimen.

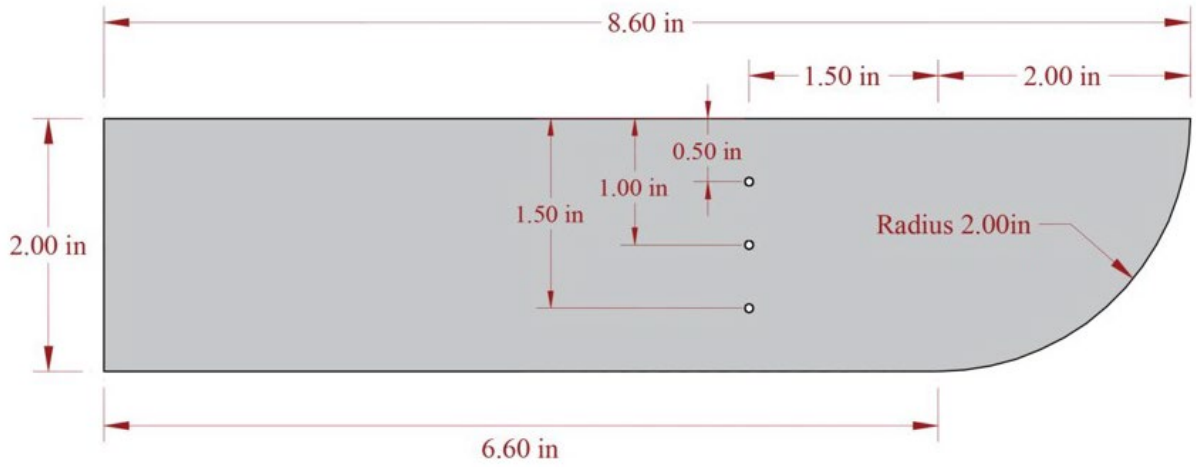

Figure 6. Engineering drawing of calibration specimen. Dimensions shown are in inches

4.2.2 Delay Lines

Delay lines were manufactured from a 32 mm cast acrylic rod to provide a buffer against the cold temperatures that would be experienced during testing. A stainless-steel collar was fabricated to fix the delay line to the front of the transducer and suitable pressure was applied to enable efficient transfer of acoustic energy. The coupling of the delay line to the transducer was achieved using Echo Ultrasonics® Forever wedge couplant. Figure 7 shows the fabricated delay lines that were used during the extreme cold temperature non-contact UT.

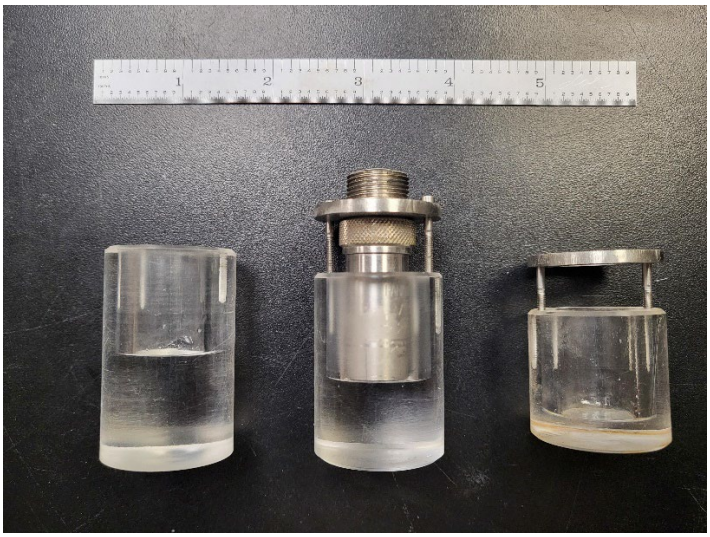

Figure 7. Delay lines used for non-contact ultrasonic testing

4.2.3 Materials

The materials tested included glycol, ultrasonic couplant, and rail steel as shown in Table 2. Glycol was also mixed with water to create different concentrations, e.g., 80/20 mix and 50/50 mix.

Table 2. List of materials tested to determine ultrasonic velocities at different temperatures

Material	Product	Notes
Glycol	Dynalene PG	Pure, 50/50 mix with water, 80/20 mix (glycol/water)
EchoPure™ MV gel	Medium viscosity ultrasonic couplant	Viscosity 35,750 centipoise (cps)
Rail steel	136 RE rail specimens	Sectioned from head/web

4.3 Density Measurements

Density changes were determined by measuring the change in volume of the liquid at different temperatures using graduated cylinders. A Fisher Scientific scale was used to measure the mass of the liquid, and the volume was determined from the graduations on the cylinder. The cylinders were placed in the immersion bath to achieve the appropriate temperature and then removed temporarily from the bath to record the volume for the given temperature. The density measurement is illustrated in Figure 8.

Figure 8. Photographs of the density measurement process, showing mass measurement (left), and the volume measurement (center, right)

5.0 RESULTS

This section describes the ultrasonic velocity, angle of refraction, and density measurements obtained for the rail steel and couplants for extreme cold temperatures. Only room temperature measurements were conducted for the baseline measurement.

5.1 Contact UT

The L-wave and S-wave velocities were first calculated at room temperature and were compared to the known values for carbon steel for verification. Once verified, velocities were calculated at temperatures ranging from -18°C to about -38°C using the same approach. The experiment was

repeated five times for each measurement group. Therefore, average velocities were calculated from each run for each temperature group. Figure 9 shows the A-scan signals for multiple back wall reflections (signal peaks) observed in a test sample using 0° L-wave transducer.

Figure 10 shows the plot for the average L-wave velocity with changing temperatures. With the help of a regression line, a slight increase in the velocity can be visualized as the temperature decreases. The difference in velocities between room temperature and -38°C is 13 m/s. This correlates to the 0.22 percent increase from the velocity obtained at room temperature to the velocity at -38°C.

Similarly, Figure 11 and Figure 12 show the plot for the average S-wave (45° and 70°) velocities with changing temperature. The velocities increased slightly as the temperature decreased. The difference in 45° S-wave velocities obtained at the room temperature and -38°C is 85 m/s. This difference corresponds to 2.61 percent increase from the velocity obtained at room temperature to the velocity at -38°C. Similarly, the difference in 70° S-wave velocities obtained at the room temperature and -38°C is 54 m/s, and this difference correlates to a 1.65 percent increase.

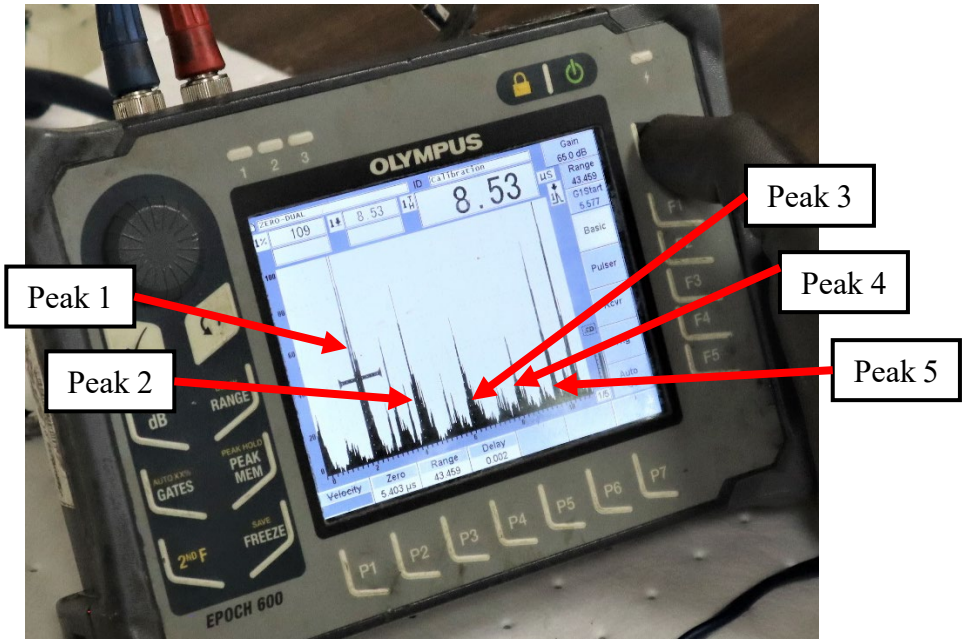

Figure 9. A-scan signal showing multiple back wall reflections in a test sample

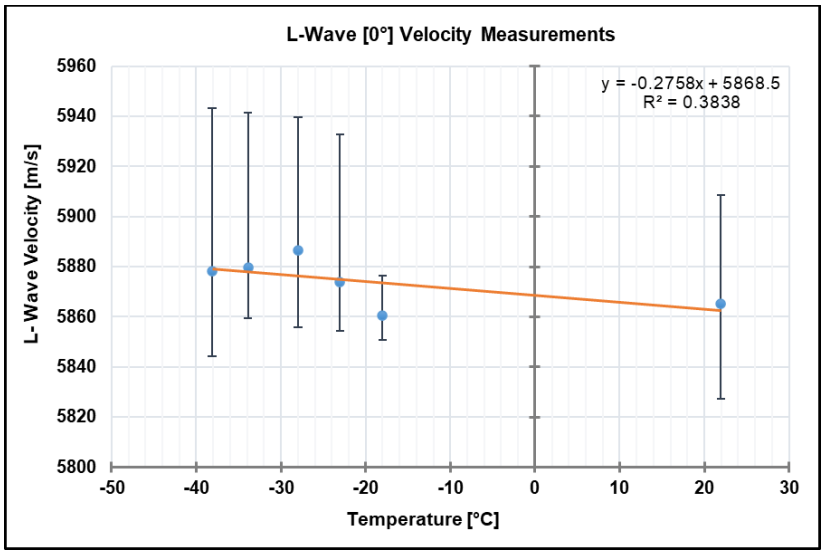

Figure 10. Rail steel L-wave velocity measurements at different temperatures for contact UT

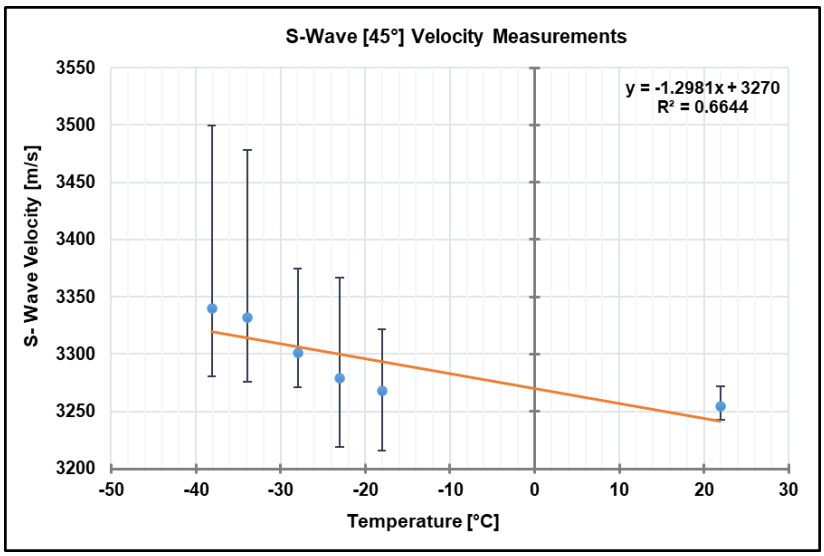

Figure 11. Rail steel S-wave (45°) velocity measurements at different temperatures for contact UT

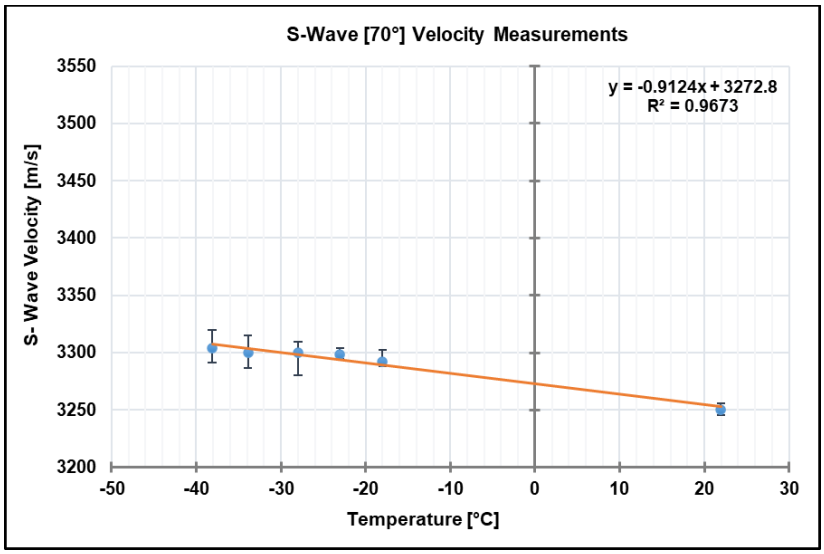

Figure 12. Rail Steel S-wave (70°) velocity measurements at different temperatures for contact UT

Data scatter was observed during most of the velocity measurements. These velocity measurements were the result of amplitude shifts (erratic readings) of the A-scans recorded and may be due to the changes in the piezoelectric crystal properties due to prolonged exposure to the lower temperature. Similar trends in outside research were observed for the high temperature testing. Therefore, future research will need to be carried out to better understand how the cold temperature affects the UT A-scan amplitudes.

5.2 Non-Contact UT

The L-wave velocity measurements for different fluids considered for this study were carried out at different temperatures using non-contact UT approach. Figure 13 shows the L-wave velocity measurements for different fluids (couplant) considered for this study. From these measurement, it was observed that the ultrasonic velocity increased with the decreasing temperatures. All velocity measurements followed the same linear trend (increasing) with the decrease in temperature.

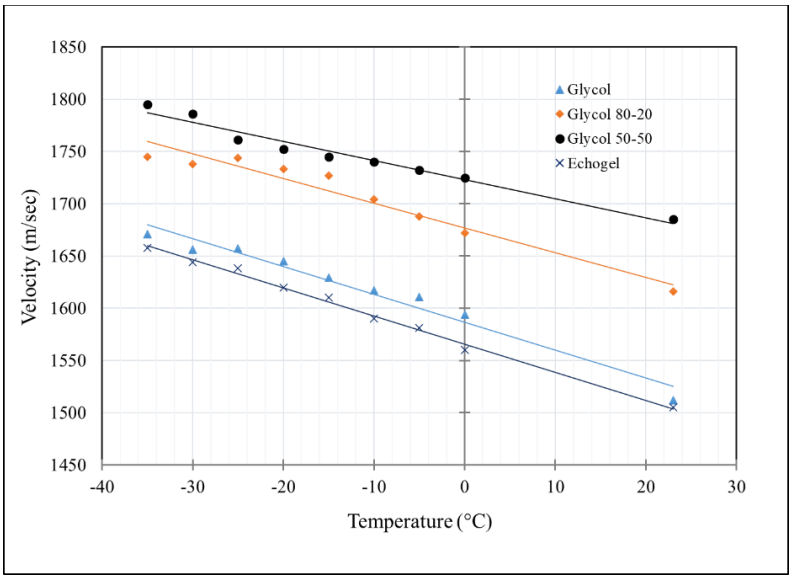

Figure 13. Fluids L-wave velocity measurements at different temperatures for non-contact UT

An assessment of the effect of temperature on the velocity of ultrasonic waves in rail steel was conducted using a non-contact UT approach. First, the L-wave velocities were measured from 23°C to -30°C. However, the measurements at temperatures of -20°C, -25°C, and -30°C appeared to be unreliable measurements. As shown in Figure 14, measurements at these temperatures departed significantly from the trend as temperatures decreased. The testing was repeated to ensure this effect was repeatable and not the result of a random error. The reduced signal-to-noise-ratio (SNR) caused by the increased ultrasonic signal losses in the liquid is believed to be the source of the apparent timing errors, resulting in what is currently believed to be inaccurate measurements of velocity. Based on the velocity measurements obtained from 23°C to -15°C, it was found that the slope of the linear regression was 0.55 m/sec/°C.

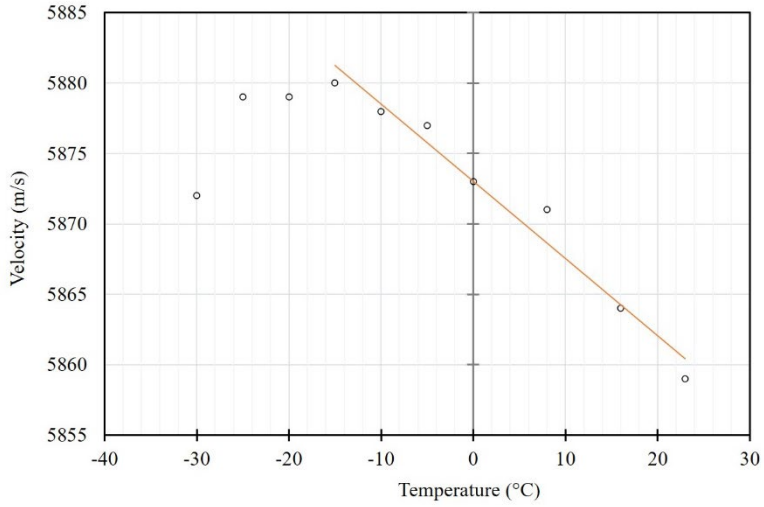

Figure 14. Rail steel L-wave velocity measurements at different temperatures for non-contact UT

Next, two sets of S-wave velocities were evaluated for refraction angles of 45° and 70°. The procedure used for an 45° S-wave were effective but proved problematic for 70° S-waves (not included) due to ultrasonic signal losses in the immersion liquid (80/20 glycol/water) as temperatures were decreased. Figure 15 shows the plot for the average S-wave (45°) velocities with changing temperature. It was found that the velocity of the S-wave increased with decreasing temperature at a rate of approximately 0.37 m/sec/°C. This value is consistent with values available in the literature of about 0.4 m/sec/°C. As a result, the initial S-wave velocity of 3212 m/sec at room temperature increased 3229 m/sec at -30°C.

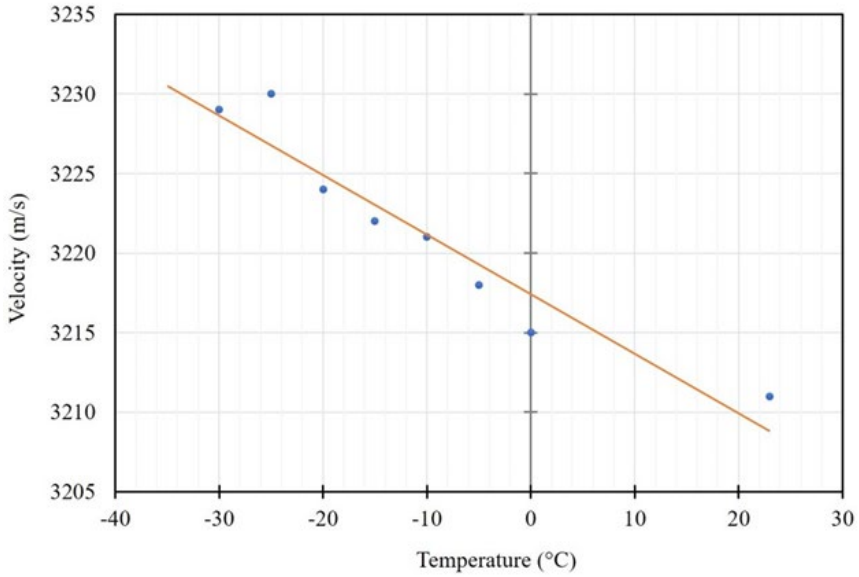

Figure 15. Rail steel S-wave (45°) velocity measurements at different temperatures for non-contact UT

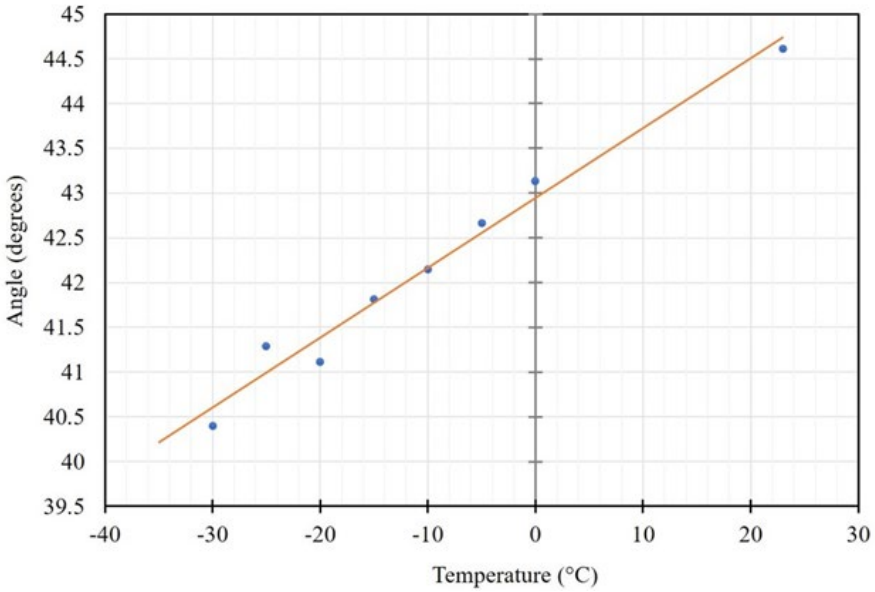

Figure 16. Rail steel 45° refraction angle variations at different temperatures for non-contact UT

Similarly, the angle of refraction was also found to vary with temperature as shown in Figure 16. As shown in the figure, the refraction angle was found to be 44.61° at the room temperature, but had reduced to 40.40° at a temperature of -30°C. The angle change as a function of temperature was found to be 0.0782°C, and the relationship was found to be linear.

5.3 Density Measurements

Density measurements for the different fluids considered for this study were also carried out at different temperatures. Figure 17 shows the density measurements for different fluids (couplant) considered for this study. It was again observed that the density increased with the decreasing temperatures.

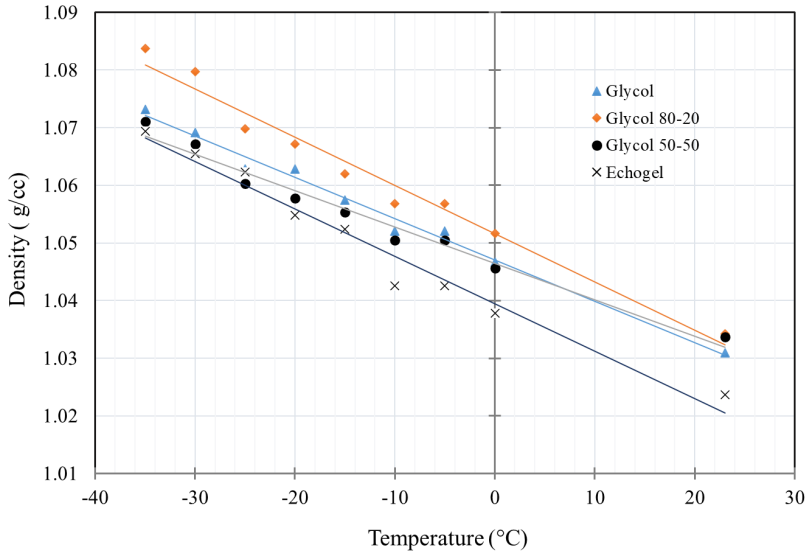

Figure 17. Density measurements for fluids at different temperatures

The velocity and density measurements for each of the liquids (couplants) tested are summarized in Table 3.

Table 3. Velocity and density slope measurements for fluids tested based on linear regression

Material	Velocity Slope (m/s/°C)	Correlation. Coefficient (R^2)	Density Slope (g/cc/°C)	Correlation. Coefficient (R^2)
Glycol	-2.66	0.97	-0.0007	0.97
Glycol/water (80/20)	-2.36	0.95	-0.0008	0.95
Glycol/water (50/50)	-1.83	0.97	-0.0006	0.97
EchoPure™ gel	-2.70	0.99	-0.0008	0.99

5.4 Ultrasonic Signal Loss Measurements

To assess the ultrasonic signal loss in the immersion liquid (50/50 water/glycol), measurements using the same setup parameters were compared using two different temperatures. The amplitudes of the SDH reflection from an incident 45° S-wave at -5°C and -20°C were compared. Figure 18a illustrates the ultrasonic signal losses in the glycol/water liquid where the specimen was immersed during testing. The data in the plot were determined by normalizing the signal amplitude in dB to the reflection from the SDH at a 13 mm depth. As shown in the figure, the loss in ultrasonic signal amplitude from the first SDH was 4.8 dB or about a 40 percent loss in signal amplitude. These losses resulted primarily from the immersion liquid in which the specimen was placed. As compared with the critical angle, the loss of transfer efficiency caused by the changes in the incident angle also contributed to this measurement, since the measurement relies on a signal reflected from within the steel. In other words, less energy is transferred from the liquid into the steel when the angle diverges from the critical angle of 45°. As a result, less energy is available to be reflected by the SDH. The contribution from this effect is likely small compared with the losses in the liquid itself.

To examine the attenuation losses in the steel, the same data was normalized to the reflection from the top SDH at a depth of 13 mm. This data illustrated the attenuation in the steel itself. These data are shown in Figure 18B. As shown in the figure, the attenuation losses in the steel are increased at the lower temperature, as illustrated by the slope of the lines and the linear regression data shown in the figure. For example, losses in amplitude were shown to be approximately -0.21 dB/mm at -20°C as compared with -0.19 dB/mm at -5°C.

The phenomena of increased attenuation in both the liquid and the rail steel itself may be worthy of further study. Very little data is available in the literature to document this effect. Practically, the ultrasonic signal losses will impact damage detection in the field by reducing the amplitude of signals as compared to the threshold value identified to determine if a given signal represents a reportable indication. The experimental results reported here were developed from the data on ultrasonic velocities; additional detailed testing is needed to characterize attenuation changes as a function of temperature.

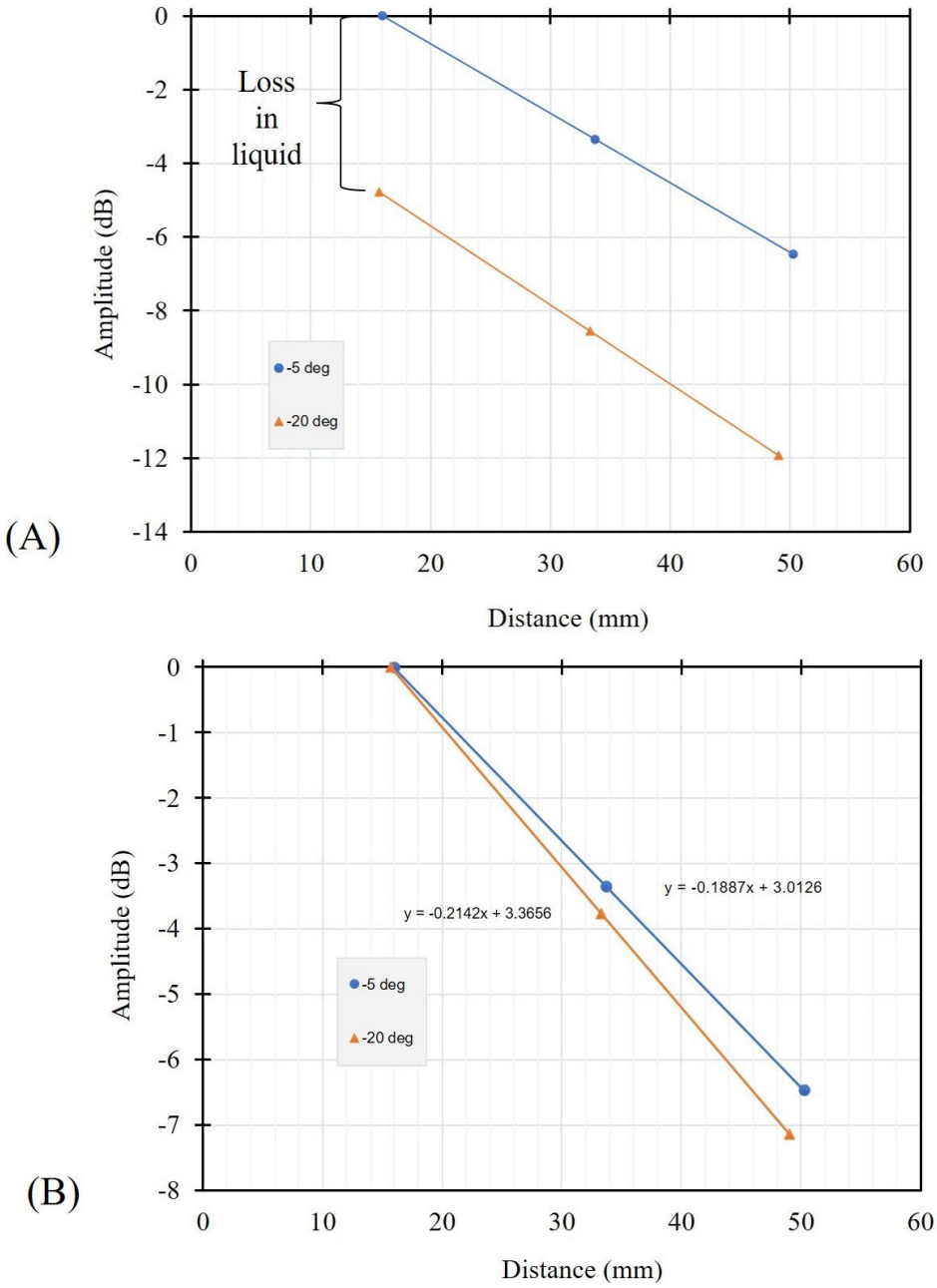

Figure 18. Losses in signal amplitude in the immersion liquid based on reflections from SDHs at 13 mm depth. (A) Amplitude loss (dB); (B) Attenuation (dB)

6.0 ULTRASONIC BEAM MODELNG AND SIMULATION

Ultrasonic beam modeling and simulation were conducted to assess ultrasonic beam field responses for the range of ultrasonic velocities and densities determined for different cold temperatures. The ultrasonic beam modeling and simulation were conducted using CIVA UT software. Details on the theory for ultrasonic beam field modeling/simulation and assumptions are reported in the literature.[13] Two-dimensional computer aided design rail models for 136RE template rail were considered for this study. The ultrasonic parameters for modeling and

simulation were chosen to closely match the parameters currently being used in the commercial detector cars. Table 4 shows some of the ultrasonic parameters considered to carry out this UT modeling and simulation work in CIVA UT.

Table 4. Ultrasonic parameters used for UT beam modeling and simulation

UT Simulation Parameters	0°	37.5°	70° Center
Pattern: Single or dual element	Single	Single	Single
Shape: Rectangular or circular	Rectangular	Rectangular	Rectangular
Dimension: Length/width/diameter [mm]	13/6	13/13	13/13
Apodisation (%)	None	None	None
Focusing Type: Flat/cylindrical/spherical	Flat	Flat	Flat
Wave Type: L-wave or S-wave	L-wave	S-wave	S-wave
Probe type:	Immersion	Immersion	Immersion
Signal type: Gaussian or Hanning	Hanning	Hanning	Hanning
Center frequency [MHz]	3.50	2.25	2.25
Bandwidth	60% @ -6 dB	60% @ -6 dB	60% @ -6 dB
Phase	0°	0°	0°
Sampling frequency [MHz]	80	80	80
Number of points	1,024	1,024	1,024
Location/positioning	Center	Center	Center
Offset from the centerline of the rail (in.)	0	0	0
Water path distance (mm)	25	25	25
Deflection (degrees)	0°	0°	0°
Rotation (degrees)	90°	90°	90°

Material properties and ultrasonic velocities for rail steel and fluids determined from the tests conducted (see the previous sections of this report) were used for UT beam modeling and simulation. Table 5 lists these values. The following assumptions were made for the values listed in this table. The density of steel was kept constant for rail steel for all temperatures. Three temperatures were considered for simulation, including room temperature (22°C) and two extreme cold temperatures (-20°C and -30°C).

Table 5. Material properties and ultrasonic velocities for rail steel and fluids used for UT modeling

Temperature [°C]	Materials	Ultrasonic Wave Velocity [m/s]		Density [g/cc]
		C_L	C_S	ρ
22	1020 Carbon Steel	5,900	3,230	7.8
22	Water	1,483	N/A	1
22	Rail Steel	5,859	3,212	7.8
22	Glycol 80/20 Mix	1,616	N/A	1.034
-20	Rail Steel	5,879	3,224	7.8
-20	Glycol 80/20 Mix	1,733	N/A	1.067
-30	Rail Steel	5,880	3,229	7.8
-30	Glycol 80/20 Mix	1,745	N/A	1.084

Figure 19 shows the probe signal modeled for 3.5 MHz 0° and 2.25 MHz 70° transducers. The sampling frequency and number of data points are important factors for achieving better quality digitized signals during analog-to-digital conversion. For this simulation, the sampling frequency was set to 80 MHz, and the number of data points was set to 1024 to obtain better digitized signals. The Nyquist limit (absolute minimum sampling requirement) states that more than two samples must be taken per period to reproduce a sinusoidal wave by sampling the analog wave. The choice of low sampling frequency might lead to loss of signal information while a high sampling frequency increases storage and computation, therefore the identification of the appropriate sampling frequency and data points is a critical factor for onset determination.

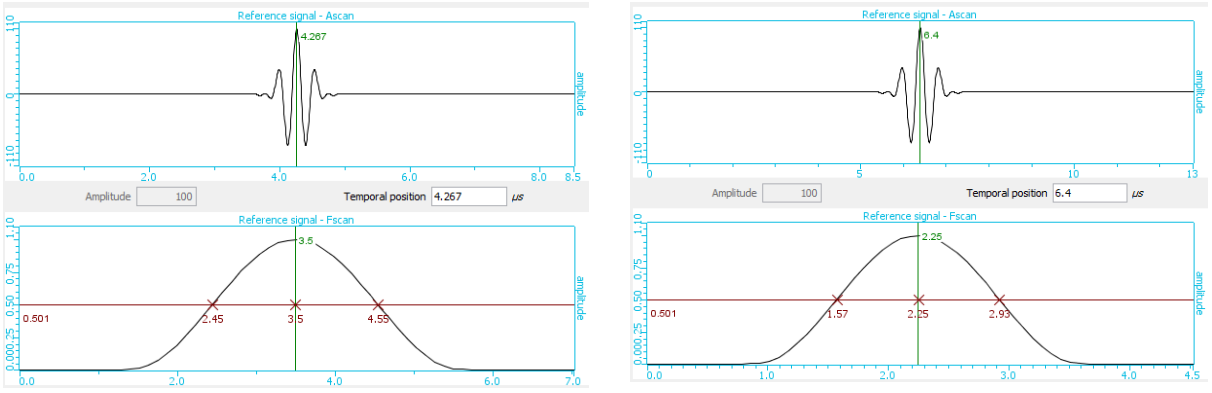

(a) (b)

Figure 19. Modeled signal in CIVA UT: (a) 3.5 MHz 0° transducer; (b) and 2.25 MHz 70° transducer

Similarly, the probe positioning inside the RSU (with fixed probe diameter and frequency) also plays an important role for optimal inspection. As a general rule, the water path distance should be in excess of 25 percent of the maximum beam path in the material for L-wave inspection and at least 50 percent of the beam path for S-wave inspection. However, for the work reported here, the water path distance was set to 25 mm for all simulations. Figure 20 shows the water path distances for the 0°, 37.5°, and 70° transducers.

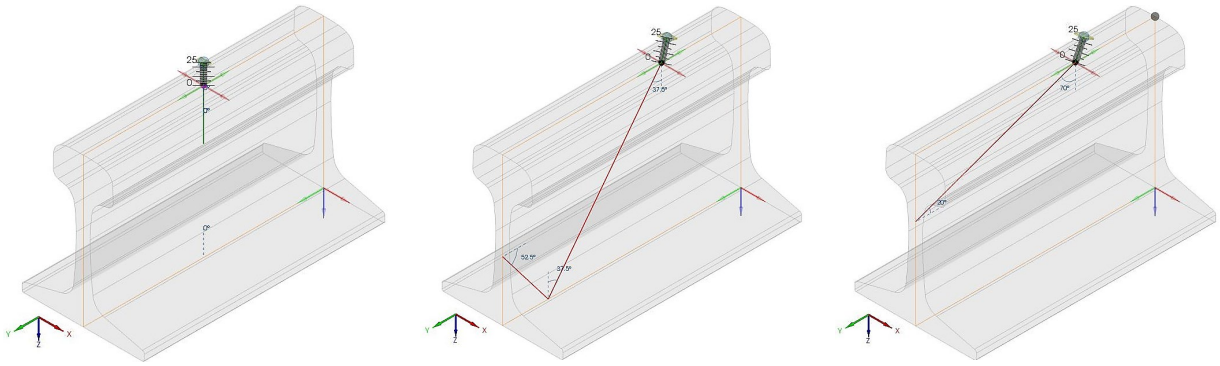

(a) (b) (c)

Figure 20. Water path distances for different transducers: (a) 0°; (b) 37.5°; and (c) 70°

The velocity of sound waves in different materials governs the angle of refraction when a wave is transmitted from one material to the other, and this effect was evident in the modeling. A summary of the refraction angle calculated for different temperatures is shown in Table 6. Also, the refraction angle for the water/steel interface is calculated and serves as a baseline for comparison under different scenarios. The results shown in Table 6 are also plotted in a graph as shown in Figure 21. The refraction angle shows the decreasing linear trend with a regression value of 0.98 for both cases. This shift in the angle of refraction can shift the beam away from the targeted inspection zone causing the beam to possibly miss defects in that zone during the inspection process. Based on this shift, performing hi-rail ultrasonic system calibration at cold temperatures while performing testing at the cold temperatures is highly recommended to when.

Table 6. Refraction angle changes in fluid/steel interface as a result in temperature change

Mediums	Incident Angle [degrees]	Refraction Angle [degrees]
Water/Steel (standard/ 22°C)	18.95	45.00
Glycol/Steel (22°C)	18.95	40.19
Glycol/Steel (-20°C)	18.95	37.16
Glycol/Steel (-30°C)	18.95	36.92
Water/Steel (standard/ 22°C)	25.56	70.00
Glycol/Steel (22°C)	25.56	60.28
Glycol/Steel (-20°C)	25.56	53.38
Glycol/Steel (-30°C)	25.56	52.97

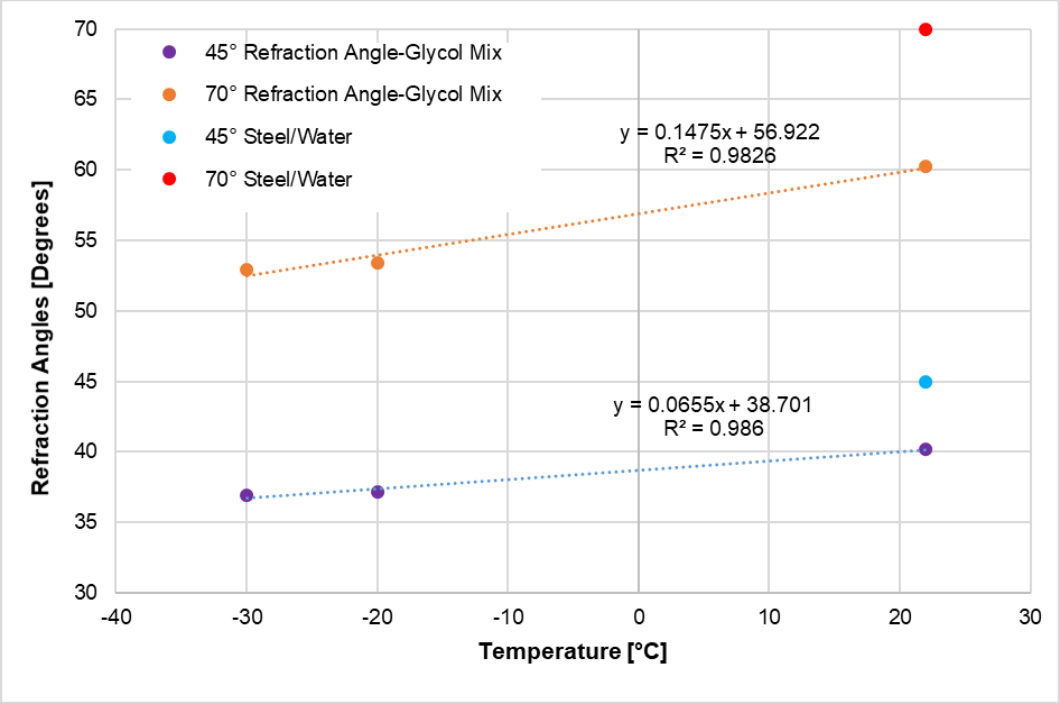

Figure 21. Refraction angle changes in fluid/steel interface as a result in temperature change

Figures 22 and 23 show the visualization of the ultrasonic S-wave beam field in rail steel for different temperatures. Although the ultrasonic beam field gets stronger based on the travel direction, a shift in the angle of refraction can cause failure to detect certain internal flaws due to the shifting of the beam from the targeted inspection zones.

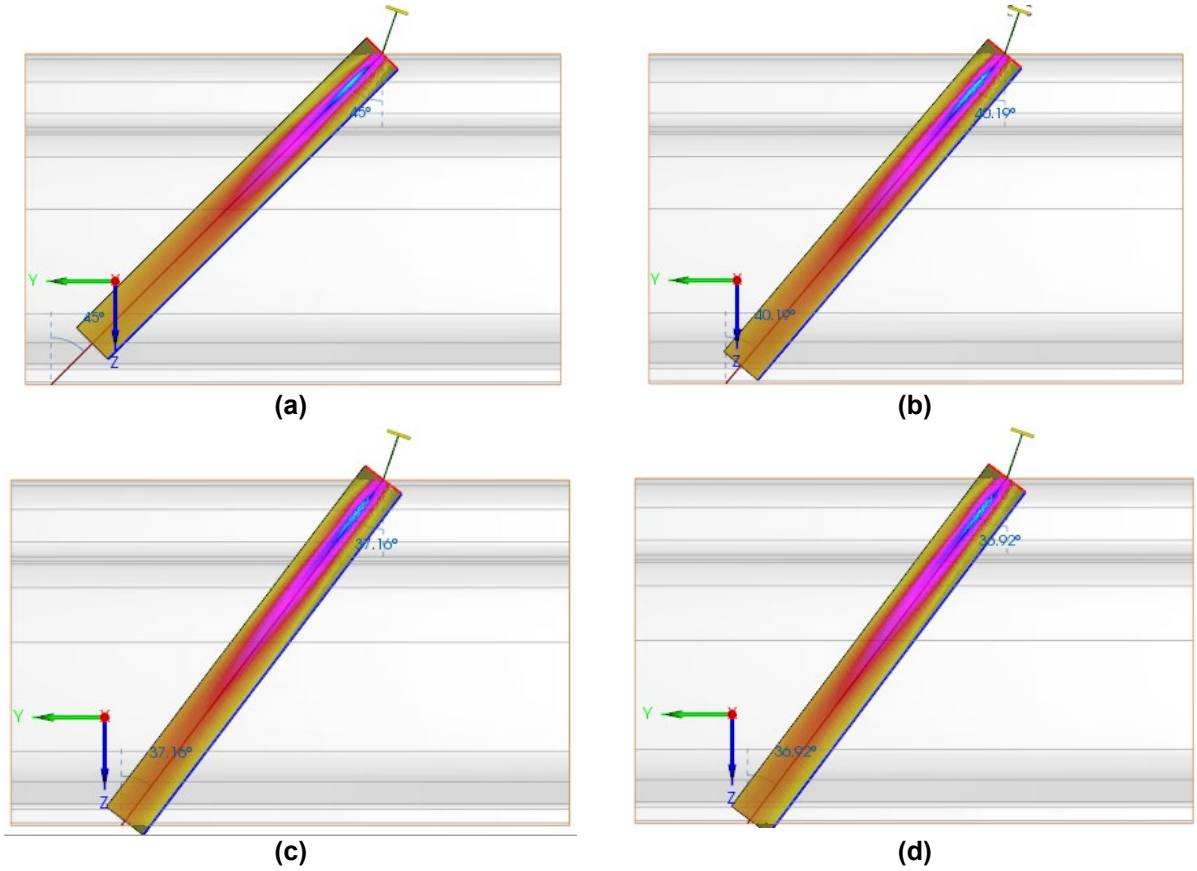

Figure 22. 45° S-wave beam field in rail steel: (a) water/steel at 22°C; (b) glycol mix/rail steel at 22°C; (c) glycol mix/rail steel at -20°C; (d) glycol mix/rail steel at -30°C

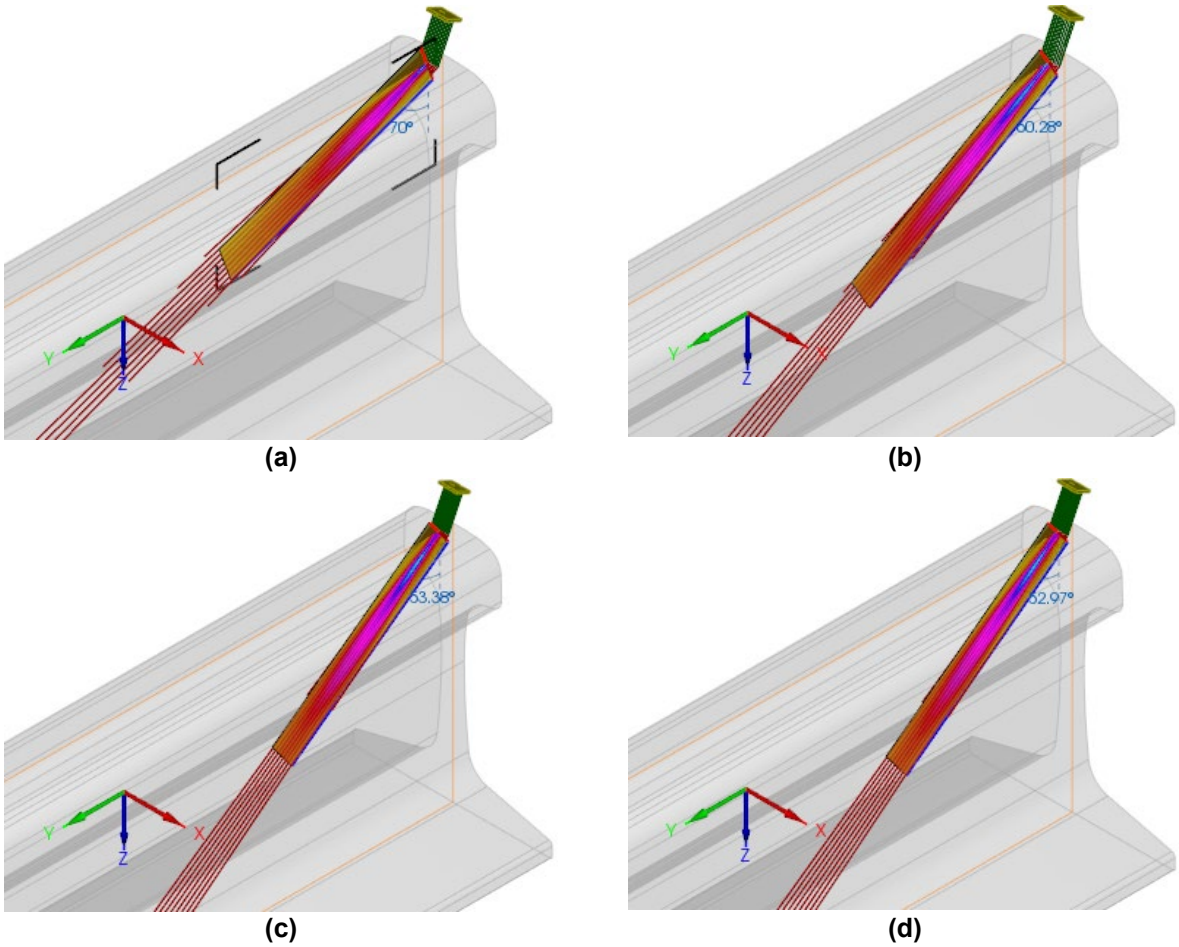

Figure 23. 70° S-wave beam field in rail steel: (a) water/steel at 22°C; (b) glycol mix/rail steel at 22°C; (c) glycol mix/rail steel at -20°C; (d) glycol mix/rail steel at -30°C

Finally, transverse fissure (TF), a type of transverse defect, inspection simulations were also conducted for different temperatures using a 70° transducer. The flaw details of the simulated flaw are shown in the Table 7. Scanning was performed along the longitudinal direction at a 1-mm step. A half-skip simulation was conducted to observe the beam interaction with the TD flaw. In UT, half-skip refers to the surface distance from the "probe index point" to the surface point above the location where the sound beam reaches the back wall of the component. In this approach, CIVA calculates contributions from a maximum of three successive skips on the specimen (external surface) and the flaw.

Table 7. Modeled TD dimensions and features

FRA Cause Codes	Defect Type	Location	Shape	Size	Orientation	Depth
T 220	TF	Center	Circular	13-mm diameter	10°	13 mm

Figure 24 shows ray tracing results for the TF defect in the rail head. All other simulations, except for the water/steel simulation, completely miss this flaw due to the change in the refraction angle. Similarly, Figure 25 shows the calibrated B-scan results for the TF inspection simulation.

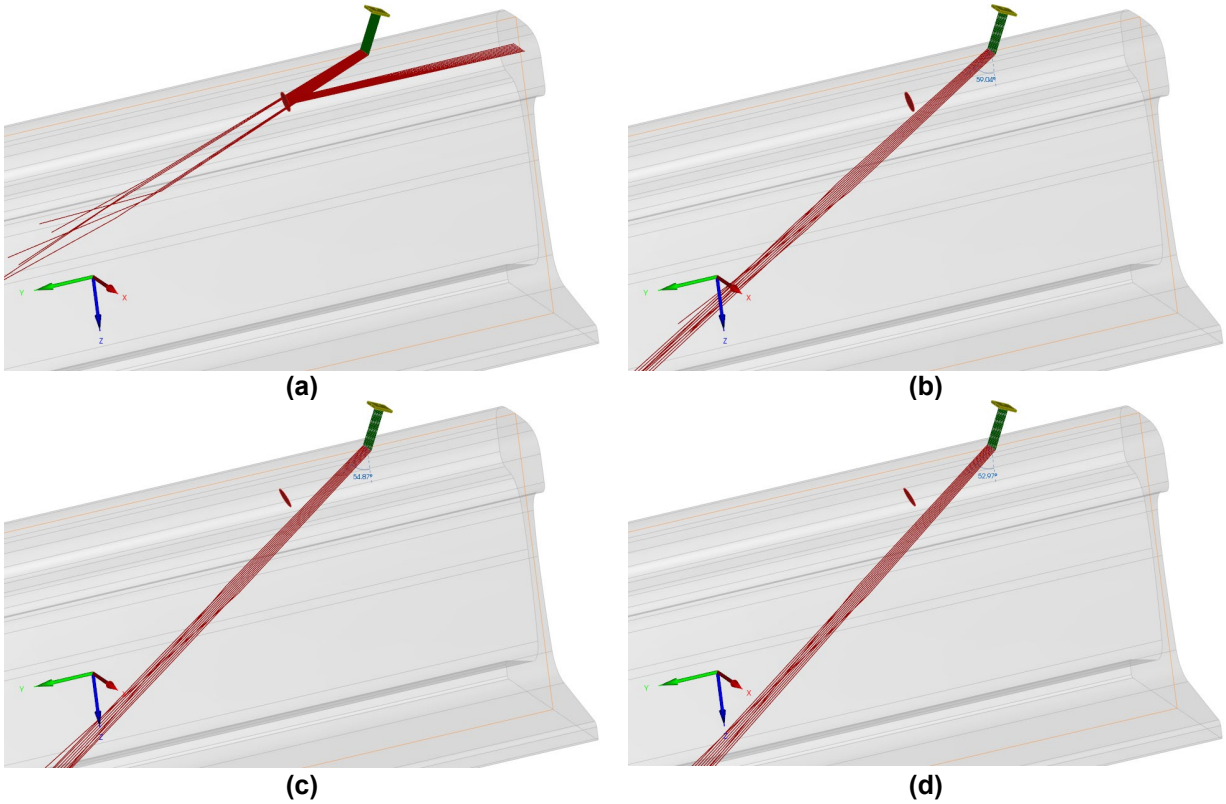

Figure 24. 70° S-wave beam ray-tracing result for TF in rail steel: (a) water/steel at 22°C; (b) glycol mix/rail steel at 22°C; (c) glycol mix/rail steel at -20°C; (d) glycol mix/rail steel at -30°C

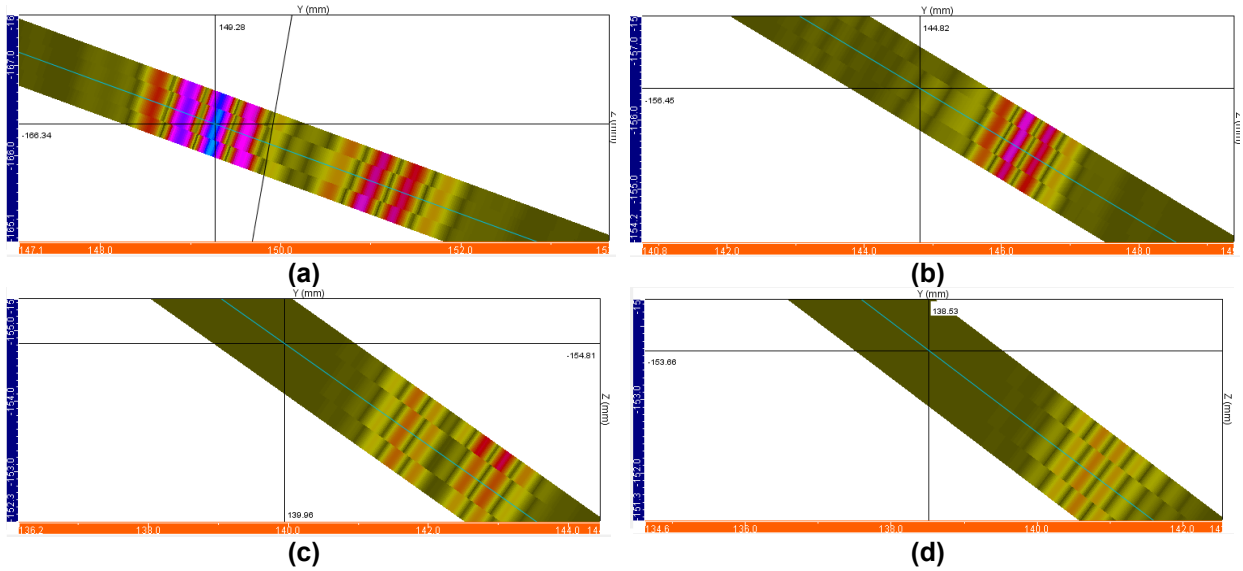

Figure 25. 70° S-wave B-scan result for TF in rail steel; (a) water/steel at 22°C; (b) glycol mix/rail steel at 22°C; (c) glycol mix/rail steel at -20°C; (d) glycol mix/rail steel at -30°C

The calibration of the test results was done using a 1.6 mm SDH located 19 mm from the top of the rail head. As shown in the results, only the initial simulation of the steel/water interface was able to detect this defect while the rest of the simulation shows this defect is completely missed at the cold temperature due to the change in the refraction angle. The maximum signal intensity observed in the B-scan due to the TF flaw for steel/water simulation had only 0.7 dB loss from the reference value and occurred at depth of 19 mm from the top of the rail head (or 166 mm from the base). The signal response observed in the B-scan for other simulations was due to the reflection from head-web fillet region not the TF defect. This was also true for the glycol mix/rail steel simulation at 22°C. The B-scan in UT refers to the image produced when the data collected from an ultrasonic inspection is plotted on a cross-sectional view of the component.

7.0 CONCLUSIONS

The cold winters in Canada bring unique challenges while maintaining the Canadian railway system. This research investigated the UT parameters associated with the ultrasonic rail flaw testing as related to extreme cold conditions. The specific objective of this research was to assess the effect of extreme cold temperatures on the velocity of ultrasound in couplants and rail steel. The research measurements were intended to provide data on densities and ultrasonic wave velocities at temperatures ranging from -40° C to 0° C. The effect of extreme cold temperatures on the refraction angle of ultrasonic waves was also examined. Some of the key findings of this research include:

Contact UT Tests

- Average L-wave velocity determined at room temperature was 5,865 m/s and at -38°C was 5,878 m/s. This corresponds to a 0.22 percent change of L-wave velocity and a linear velocity increase trend.
- Average S-wave (45°) velocity determined at room temperature was 3,255 m/s and at -38°C was 3,340 m/s. This corresponds to 2.61 and a linear velocity increase trend.
- Average S-wave (70°) velocity determined at room temperature was 3,251 m/s and at -38°C was 3,304 m/s. This corresponds to 1.65 percent change and a linear velocity increase trend was linear.
- Data scatter was observed during most of the velocity measurements. These velocity measurements were a result of amplitude shifts (erratic readings) of the A-scans recorded and may be due to changes in the piezoelectric crystal properties due to prolonged exposure to the lower temperature. Similar trends in outside research for the high temperature testing were also observed. Therefore, future research will need to be carried out to better understand how the cold temperature affects the UT A-scan amplitudes.

Non-Contact UT Tests

- Ultrasonic velocity increased with decreasing temperature for all fluids tested. All velocity measurements followed the same linear trend (increasing) with the decrease in temperature.
- L-wave velocities for rail steel were measured from 23°C to only -30°C. Temperatures below -30°C were not achievable in the chiller batch.
- L-wave velocity measurements for rail steel at temperatures of -20°C, -25°C, and -30°C were not consistent with the overall trend velocity increasing as temperature decrease which may have been due to the increased ultrasonic signal losses in the liquid resulting in reduced signal-to-noise-ratio (SNR) leading to timing errors in the received signal. Average L-wave velocity determined at room temperature was 5,859 m/s and at -30°C was 5,880 m/s. This corresponds to velocity increase of 0.55 m/sec/°C.
- The procedure used for a 45° S-wave was effective but again proved problematic for 70° S-waves due to ultrasonic signal losses in the immersion liquid (80/20 glycol/water) as temperatures were decreased.
- Average S-wave (45°) velocity determined at room temperature was 3,212 m/s, at -20°C was 3,224 m/s, and at -30°C was 3,229 m/s. The change in average S-wave velocity corresponds to velocity increase approximately 0.37 m/sec/°C.
- A 45° refraction angle change as a function of temperature was found to correspond with 0.0782 deg/°C, and the relationship was found to be linear.
- Signal attenuation losses in the steel increased at the lower temperature. For example, losses in amplitude were shown to be about -0.21 dB/mm at -20°C as compared with -0.19 dB/mm at -5°C. The phenomena of increased attenuation in both the rail steel and the liquid couplant may be worthy of further study. Very little data is available in the literature to document this effect. Practically, the ultrasonic signal losses will impact damage detection in the field by reducing the amplitude of signals as compared to a threshold value identified to determine if a given signal represents a reportable indication.

Signal attenuation losses were developed from the data on ultrasonic velocities; additional detailed testing is needed to characterize attenuation changes as a function of temperature.

- Signal attenuation losses in the steel increased at the lower temperature. For example, losses in amplitude were shown to be about -0.21 dB/mm at -20°C as compared with -0.19 dB/mm at -5°C. Signal attenuation losses were developed from the data on ultrasonic velocities; additional detailed testing is needed to characterize attenuation changes as a function of temperature.

UT Beam Modeling and Simulation

- Ultrasonic beam modeling and simulation were conducted to assess ultrasonic beam field responses for the range of ultrasonic velocities and densities determined for different cold temperatures.
- Velocity of the sound waves in different materials governs the angle of refraction when a wave is transmitted from one material to the other, and this effect was evident in the modeling. The refraction angle shows a decreasing linear trend with a linear regression value of 0.98 for both cases. This shift in the angle of refraction can cause the beam to shift away from the targeted inspection zone, a shift that can cause the beam to possibly miss defects in that zone during the inspection process. Based on this possibility to angle of refraction shifts, it is highly recommended to perform hi-rail ultrasonic system calibration at cold temperatures when performing testing at cold temperatures.
- All other simulations conducted for extreme low temperatures, except for water/steel simulation at room temperature, failed to detect transverse type defects. This failure was a result of the change in the refraction angle.

Several challenges were encountered with performing measurements over this temperature range, but generally, two challenges that affected testing were also encountered. First, the minimum achievable temperature in the laboratory was found to be -35°C for liquids and -30°C for steel measurements. Second, unexpectedly high losses in the immersion liquid were experienced and precluded reliable measurements in some cases. In spite of these challenges, data shown in the report included velocity and density measurements for the liquids under study from 23°C to -35°C. For the rail steel, measurements were reported for S-wave velocities and refraction angles from 23°C to -30°C, based on a 45° refracted wave. Refraction angle changes for a 45° S-wave are also reported, along with longitudinal wave velocity data from 23°C to -30°C. However, some of these measurements were not considered to be accurate, as discussed in the report. Limited data on the attenuation of ultrasonic waves in liquids and steel are presented to illustrate a future research need.

References

1. Garcia, G. and Jeong, D. Y., 2003, “Rail Defect Growth Under Heavy Axle Loads,” Railway Track and Structures, Simmons-Boardman Publishing Corporation, New York, NY, pp. 17–19.
2. Orringer, O., Morris, J. M., and Jeong, D. Y., 1986, “Detail Fracture Growth in Rails: Test Results, ” Theoretical and Applied Fracture Mechanics, 5(2), pp. 63–95.
3. Banerjee, A. and Morrison, K., 2019, “Fatigue Crack Growth Rate Properties of Rail Steels and Their Influence on Rail Life,” *Technology Digest*, TD-19-008. AAR/TTCI, Pueblo, CO.
4. Stenström, C., Famurewa, S., Aditya, P., and Galar, D., “Impact of Cold Climate on Failures in Railway Infrastructure, ” Proc. 2nd International Congress on Maintenance Performance Measurement & Management.
5. Ladubec, C. and Magel, E., “Winter Railroading in Canada - A Review of Track and Rolling Stock Challenges, ” Proc. International Heavy Haul Association Conference.
6. Poudel, A., Lindeman, B., and Wilson, R., 2019, “Current Practices of Rail Inspection Using Ultrasonic Methods: A Review, ” Materials Evaluation, 77(7), pp. 870–883.
7. Alahakoon, S., Sun, Y. Q., Spiryagin, M., and Cole, C., 2017, “Rail Flaw Detection Technologies for Safer, Reliable Transportation: A Review, ” Journal of Dynamic Systems, Measurement, and Control, 140(2).
8. Robin, C., 2004, “Rail Flaw Detection: Overview and Needs for Future Developments, ” NDT & E International, 37(2), pp. 111–118.
9. U.S. Code of Federal Regulations, 49 CFR Part 213.240, 2020, “Continuous Rail Testing, ”, Federal Railroad Administation, ed., USDOT, Washington DC.
10. U.S. Department of Transportation, 2021, “Federal Railroad Administration Announces Rail Inspection Technology Rule to Improve Track Safety,” Office of Public Affairs, Washington, DC.
11. Rose, J. L., 2014, Ultrasonic Guided Waves in Solid Media, Cambridge University Press, Cambridge.
12. Josef, K. and Herbert, K., 1990, Ultrasonic Testing of Materials, Springer Berlin Heidelberg, Germany.
13. Gao, Y., Poudel, A., and Lindeman, B., 2021, “Automated Broken Spike Detection – Phase I, ” Federal Railroad Administration, ed., Washington, DC.